Cancer Imaging (2009) **9,** 70–81
DOI: 10.1102/1470-7330.2009.0012

REVIEW

Imaging 'the lost tribe': a review of adolescent cancer imaging. Part 1

P.D Humphries and I. Zerizer

University College London Hospital NHS Trust, 235 Euston Road, London, NW1, UK

Corresponding address: Dr P.D. Humphries, Specialist X-ray, Podium Level 2, University College London Hospital NHS Trust, 235 Euston Road, London, NW1, UK.
Email: paul.humphries@ulch.nhs.uk

Date accepted for publication 10 August 2009

Abstract

Although a small proportion of all cancer registrations, malignancy in adolescence and young adulthood remains the most common natural cause of death in this age group. Advances in the management and outcomes of childhood cancer have not been matched within the adolescent population, with increasing incidence and poorer survival seen amongst teenagers with cancer compared with other populations. There have been increasing moves towards specific adolescent oncology centres, with the aim of centralising expertise, however, 'adolescent imaging' does not exist as a speciality in the same way that paediatric imaging does, with responsibility for imaging adolescent patients sometimes falling to paediatric radiologists and sometimes to 'adult' radiologists, usually with a specific interest in a tumour type or body system. In this article, imaging of the more common malignancies, encountered in adolescent patients is reviewed. Complications of treatment are reviewed in another article to give an overview of adolescent oncology imaging practice.

Keywords: *Adolescent; oncology; lymphoma; bone tumour; carcinoma.*

Introduction

Paediatric oncology is, by its very nature, a unique and distinctly different medical speciality to all other oncological practice. In contrast to an organ system-based division of tumour types as in adult practice, paediatric oncology is an age-based speciality, with a wide variety of different tumours seen within this group of patients. Not only are the tumours encountered within paediatric oncology a varied group, but the patients themselves are also a heterogeneous group, ranging from the newborn to the teenager, and possibly beyond. There are various definitions of what constitutes 'paediatric' or 'adolescent' patients, and the terms 'children', 'teenagers' and 'young people' are sometimes used loosely. In its guidance *Improving Outcomes in Children and Young People with Cancer*, the National Institute for Health and Clinical Excellence regards those aged less than 15 years as children, and those aged from 15 to 24 as young people[1]. In the United Kingdom, the Children's Cancer and Leukaemia Group (http://www.cclg.org.uk) reports patients aged up to 15 years separately from those older than 15 years, with the National Registry of Childhood Tumours (http://www.ccrg.ox.ac.uk) registering all malignancies (and benign brain tumours) in patients less than 15 years living in the United Kingdom at the time of diagnosis. The spectrum of malignant diseases in adolescence and early adult life is different from that in any other period in life, and it is strikingly different from the pattern in adults and that seen in younger children[2]. More people 15–25 years of age are diagnosed to have cancer than during the first 15 years of life. During the last 25 years, the incidence of cancer in this age range has increased faster and survival rates have been significantly lower than in younger or older patients[2–5]. The transition from child to adolescent and adolescent to young adult is of course a continuum, with gradually changing needs and can be daunting. Adolescent oncology patients have in the past fallen between age inappropriate paediatric services and

adult oncology services, leading to the description of adolescent oncology representing the 'lost tribe'[6]. The 'lost tribe' have in recent years found a home, with 8 dedicated teenage cancer centres now established within the United Kingdom.

This article reviews the imaging features of the most common adolescent and early adulthood cancers.

Types of cancer

There are approximately 1400 new cases of malignancy diagnosed in children (age 0–14 years) per year in the United Kingdom, with 27.9% occurring in the 10–14 years age group (The National Registry of Childhood Tumours, 2000 data). Cancer incidence rates for adolescents and young adults are not included in the National Registry of Childhood tumours data and the most recent resource available is a report by Birch *et al.*[7] documenting the incidence of malignant disease by morphologic type in patients age 12–24 years for the period 1979–1997. Most of the common 'developmental' malignancies in children younger than 5 years of age, including the embryonal malignancies such as Wilms tumour, neuroblastoma and hepatoblastoma, are uncommon in adolescents and young adults, for example with only 40 cases of Wilms tumour seen in the age range 12–24 years in the entire study period. The incidences of malignant bone tumours, germ cell tumours, and lymphoma have a peak in incidence during adolescence and young adulthood. Central nervous system tumours are seen less frequently than in children less than 10 years, but still accounted for 2.9% of new cancer cases. Astrocytoma is the most common tumour observed, with a trend towards higher grade tumours with increasing age. Although a significant proportion of adolescent oncology workload, given the childhood predominance of central nervous system (CNS) tumours, astrocytomas are not discussed further in this review. Adolescents and young adults are less likely to develop the cancers that predominate in older adults, such as carcinomas of the gastro-intestinal and genito-urinary tracts; however these malignancies can be seen.

Lymphoma

Lymphoma shows a marked increase in incidence with increasing age, being the most common cancer affecting 15–24 year olds[7] (20% of all cases), with Hodgkin lymphoma (HL) alone accounting for 12% of all new cancer diagnoses in this age group. Rates for HL and non-Hodgkin lymphoma (NHL) show steady increases with increasing age, with HL being approximately 3 times more common in the 20–24 year age group than 12–14 years[7].

Lymphoma typically presents as painless lymphadenopathy, with or without systemic symptoms such as fever, night sweats and weight loss. A mediastinal mass may be found incidentally on chest radiographs performed for other reasons. Pathologically HL can be divided into nodular lymphocyte predominant HL and classic HL (nodular sclerosing, lymphocyte rich, mixed cellularity or lymphocyte depleted). NHL is a more heterogeneous group, with both T and B cell lymphomas seen, including Burkitt lymphoma, lymphoblastic lymphoma and large-cell lymphomas. NHL seen in children and adolescents tends to be more aggressive and of higher grade than that seen in the adult population[8].

Lymph node enlargement can be seen as multiple, rounded soft-tissue masses or bulky soft-tissue masses caused by nodal aggregation. Usually, a homogeneous soft-tissue mass is noted, but it may be heterogeneous when it is large, with areas of low attenuation representing necrosis, haemorrhage, or cyst formation.

A mediastinal mass is a presenting feature in approximately 60–70% of cases of HL and 20% of cases of NHL[10]. HL tends to spread contiguously along lymph node chains; by contrast NHL is frequently discontiguous in its distribution. Pulmonary parenchymal involvement and mediastinal lymphadenopathy are less common manifestations of NHL than they are of HL[9].

Multiple nodules are the most common feature of lung involvement in both HL and NHL; however, poorly defined opacification with air bronchograms may also be seen. Features indistinguishable from pneumonic change, such as bilateral airspace consolidation and segmental or lobar atelectasis, are less common. Pleural involvement is characterised by nodular or plaquelike subpleural deposits of lymphomatous tissue. Pleural effusion may be caused by obstruction of the lymphatics, pulmonary veins, or thoracic duct, or as a result of direct pleural invasion. Invasion of the thoracic wall as a direct extension from mediastinal disease is more common in NHL, although primary involvement of the thoracic wall may occur. Thoracic wall involvement may appear as a destructive rib or vertebral-body lesion with a surrounding soft-tissue mass.

Liver and splenic involvement is seen in 15% and 22% of patients, respectively, in NHL[10]. Diffuse infiltrative involvement of the liver, spleen, and bone marrow cannot be accurately detected with computed tomography (CT), as organomegaly is a poor predictor of tumour involvement. In fact, approximately 30% of patients with splenic enlargement do not have malignant involvement. Sensitivity rates for CT are 15–37% for infiltrative splenic disease and 19–33% for infiltrative liver disease[10].

Staging

HL is staged using the modified Ann Arbor classification system, with the same criteria as those used in adult patients (Table 1). Because of a greater propensity toward extranodal disease and unpredictable spread in paediatric NHL compared with adult NHL, the Ann Arbor system is not used. The most commonly used

Table 1 Cotswold's Revision of the Ann Arbor Staging system.

Stage I	Single lymph node region involvement, including isolated splenic involvement
Stage II	Two or more lymph node regions involved on the same side of the diaphragm
Stage III	Lymph node groups or lymph structures involved on both sides of the diaphragm
Stage IV	Discontinuous extranodal involvement: – Liver lesions – Pulmonary lesions: nodule greater than 1 cm or >3 nodules <1 cm in size – Bone or bone marrow involvement – CNS involvement
A	Absence of 'B' symptoms
B	Presence of at least one of: a. Unexplained weight loss of more than 10% in 6 months b. Drenching night sweats c. Unexplained persistent or recurrent fever >38°C
E	Involvement of a single extranodal site in continuity with nodal disease. Except liver or bone marrow involvement (always implies stage IV disease)

Table 2 The Murphy system for staging childhood and adolescent NHL.

Stage	Features
I	Single extranodal tumour or single nodal anatomic area, excluding the mediastinum or abdomen
II	Single extranodal tumour with regional lymph node involvement 2 or more nodal areas on the same side of the diaphragm 2 single extranodal tumours with or without regional lymph node involvement on the same side of the diaphragm A primary gastro-intestinal tract tumour, with or without involvement of the associated mesenteric nodes only, grossly completely resected
III	2 single extranodal tumours on opposite sides of the diaphragm 2 or more nodal areas above and below the diaphragm All primary intrathoracic tumours, i.e. mediastinal, pleural or thymic All extensive primary intra-abdominal disease, unresectable All paraspinal or epidural tumours, regardless of other tumour sites
IV	Any of the above with CNS and/or bone marrow involvement

system for staging childhood and adolescent NHL is the Murphy system (Table 2)[11].

Imaging of lymphoma

Plain radiographs, CT, ultrasonography, magnetic resonance imaging (MRI) and positron emission tomography (PET)-CT may be used in the staging, disease response assessment and follow-up of lymphoma[12–15]. Anatomic staging is performed using cross-sectional imaging to evaluate the neck, chest, abdomen and pelvis. MRI or CT can

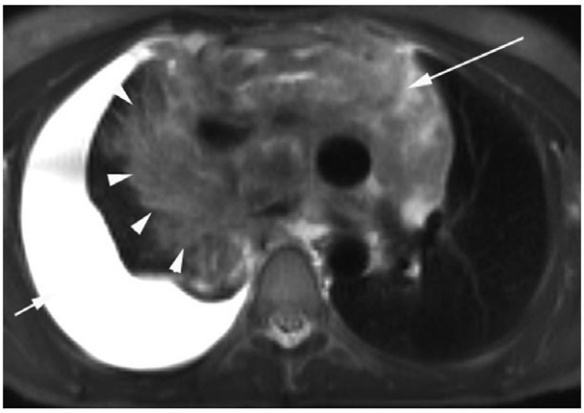

Figure 1 **Axial short time inversion recovery (STIR) MRI (TR 5.97, TE 60, TI 130 ms) of a patient with HL, showing a large mediastinal mass (long arrow), with direct lung infiltration (arrow heads) and a large pleural effusion (short arrow).**

be utilised; however the thorax should be evaluated with CT as there are no data available evaluating the effectiveness of current MRI sequences for the detection of lung parenchymal disease in lymphoma. The presence of chest wall invasion has implications for treatment, with 'E' disease if present, upstaging the patient. Bergin *et al.*[16] report a greater sensitivity for the detection of chest wall disease using MRI than that observed with CT in a group of 28 adult patients; however, the definition of chest wall disease in this series includes subpectoral nodes, with only 6 of 14 observed positive sites being contiguous with either mediastinal or pleural disease. The accuracy of MRI in the assessment of chest wall invasion in the paediatric population has not been fully evaluated, although preliminary work seems promising[17]. The use of respiratory and ECG gating (Fig. 1), possibly in combination with motion correction MR techniques such as Periodically Rotated Overlapping ParallEL Lines with Enhanced Reconstruction (PROPELLER) MR pulse sequences (e.g. Siemens 'BLADE') which can reduce motion artefact, increase signal to noise ratio, and produce sharp images even with patient motion[18], deserve further investigation.

It is well recognised that CT has a limited sensitivity and specificity for splenic visceral involvement by lymphoma[10] and there are no reports in the literature evaluating the sensitivity of MRI for the detection of splenic lesions. The spleen, therefore, should be evaluated using high-resolution ultrasound for small infiltrative lesions not apparent on CT or MRI[19]. Apart from these limitations, MRI has much to recommend it for the staging and response assessment of lymphoma in adolescents and young adults, namely, a non-ionizing means of rapidly evaluating the whole body, with increased sensitivity for bone marrow and bone lesions compared with CT and bone scintigraphy[20,21].

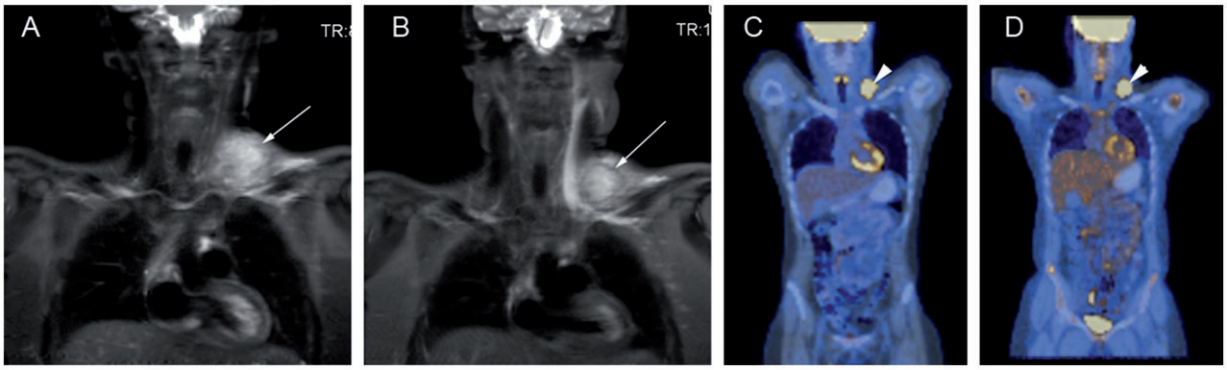

Figure 2 **Coronal STIR MRI (TR 5.97, TE 60, TI 130 ms) and PET images of a patient with HL, before chemotherapy (A,C) and following 2 cycles of OEPA chemotherapy (vincristine, etoposide, prednisolone, doxorubicin) (B,D), showing a small change in size of a left supraclavicular nodal mass (long arrows), and inadequate metabolic response (arrow heads), with persistent PET positivity.**

In addition to anatomic staging, metabolic assessment of disease is also performed at initial staging, using PET. PET is well established in adult lymphoma practice[12–14,22,23] and is now utilised in paediatric and adolescent HL. A multi-centre trial (EuroNet-PHL-C1, http://www.lymphome.de/Gruppen/GPOH-HD/Protokolle/EuroNet-PHL-C1/Synopsis.pdf) **using** metabolic response, as determined by PET response after 2 cycles of chemotherapy, is underway to decide if radiotherapy should be used at the end of treatment, with radiotherapy used in those patients who fail to show adequate metabolic response (Figs. 2 and 3). The rationale for this approach is based on evidence that metabolic response after 2 cycles of chemotherapy predicts outcome in HL[24]. Hutchings *et al.*[24] evaluated PET studies performed in 77 adult patients after 2 cycles of chemotherapy and found that 11 of 16 patients showing incomplete metabolic response progressed and 2 died during a follow-up period of 23 months. By comparison, 3 of 61 patients with complete metabolic response progressed, with no deaths in this group. For prediction of progression-free survival, re-evaluating metabolic response after 2 cycles of chemotherapy was as accurate as evaluating after 4 cycles or at the end of treatment. Re-evaluation after 2 cycles has the additional advantage of likely greater volume of disease than at end of treatment and hence a greater chance of detecting truly positive disease, as PET may be falsely negative when nodes are less than 1 cm in size. There is very little role for radiotherapy in childhood/adolescent NHL and hence PET is not used routinely to assess disease response in this population.

Functional assessment of disease using PET imparts an additional radiation burden on an individual undergoing treatment. Recent advances in MR sequences now allow functional assessment of tissue to be made. The apparent diffusion coefficient (ADC) of tissue, as derived from diffusion-weighted MR imaging (DWI) reflects the microscopic movement of water molecules within a given tissue. ADC has been shown to correlate with cell density of tissue both within the CNS[25] and within paediatric body tumours[26]. A relationship between ADC quantitative measure and the specific uptake value (SUV) of lymphomatous nodes in paediatric and adolescent patients has recently been described[27]. Further work in this group of patients to correlate ADC values after treatment with SUV and long-term follow-up is needed to determine if quantitative ADC measurements could be utilised as a non-ionizing means of determining disease response and/or relapse during follow-up.

Current guidelines for follow-up during the first year following completion of therapy encourage the use of cross-sectional imaging and ultrasound to evaluate for disease progression (defined as occurring within 3 months following end of treatment), relapse, being defined as early if between 3 and 12 months, or late relapse if occurring more than 12 months following the end of treatment. Where local expertise exists, MR has advantages over CT for follow-up, as described earlier.

Bone tumours

Primary bone tumours have a peak incidence between 10 and 20 years, with Birch *et al.*[7] reporting the rate to be highest between 12 and 19 years. Osteosarcoma (OS) accounts for most bone tumours seen amongst adolescents (approximately 55% of the total), with Ewing's family of tumours (EFT) being the next most common (approximately one-third of the total). Chondrosarcoma is seen with increasing frequency with age, being more common in the young adult age group (20–24 years) than at any other age. The more uncommon bone tumours (including malignant fibrous histiocytoma of bone and other spindle cell tumours) as a group accounted for approximately 3% of the total number of primary bone tumours seen in the 12–24 years age range[7–9].

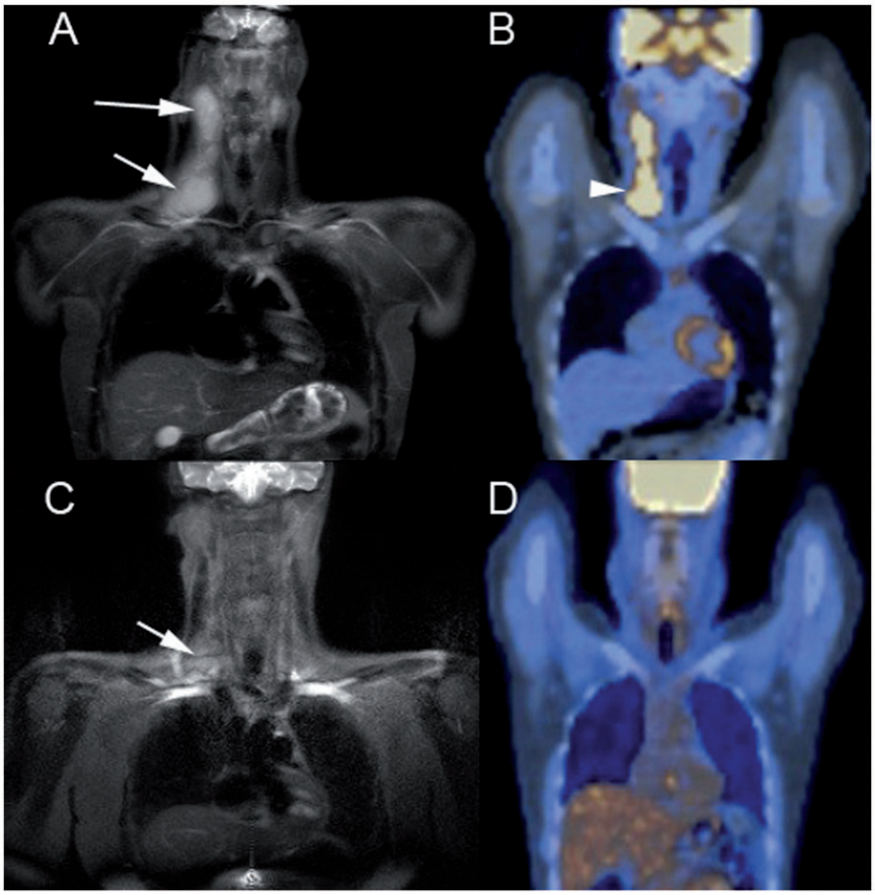

Figure 3 **Coronal STIR MRI (TR 5.97, TE 60, TI 130 ms) and PET images of a patient with HL, before chemotherapy (A,B) and after 2 cycles of OEPA chemotherapy (C,D). Initial imaging shows large volume right cervical (long arrow) and supraclavicular fossa disease (short arrow), which is PET positive (arrow head). Following 2 cycles of OEPA there is residual disease within the right supraclavicular fossa (short arrow, image C), but there is no FDG uptake, indicating an adequate metabolic response.**

OS and EFT most commonly present with pain. Typically the diagnosis is delayed as the presenting symptom is often attributed to 'growing pains' or minor trauma. Red flag symptoms include persistent night time pain or back or buttock pain. Systemic symptoms such as fever are more commonly encountered with EFT than OS. There are recognised associations with previous retinoblastoma, prior alkylating agent treatment and radiotherapy with the development of OS.

Imaging of primary bone tumours

Osteosarcoma has a proclivity for the metaphyses of long bones, with the most common site being around the knee. Plain radiograph features include an osteolytic appearance, a sclerotic appearance or a mixed appearance. Cortical destruction, periosteal reaction (which may be so rapidly increased as to produce a Codman triangle), new bone formation and a soft-tissue mass may be appreciated on the plain radiograph and suggest the diagnosis.

EFTs may also affect long bones, but are also seen affecting 'flat' bones, for example the iliac wing or ribs; indeed approximately 50% of all EFTs arise within the pelvis or the femur. Radiologically classic EFTs have a permeative 'moth eaten' appearance, with an 'onion skin' periosteal reaction (Fig. 4). Although new bone formation is the hallmark of OS, this phenomenon may also be seen in EFTs. The pelvic location of EFTs may hinder rapid diagnosis as a significant soft-tissue mass may be present without being clinically apparent.

The primary lesion should be staged for locoregional extent using MRI, the chest evaluated using CT and distant bony sites evaluated using bone scintigraphy. Locoregional MRI is used to evaluate the local tumour, with particular care taken to assess which muscle compartments are involved, the relationship of the tumour to neurovascular structures and to determine epiphyseal involvement, as these factors are important for biopsy and surgical planning. Percutaneous biopsy should be performed at a designated bone tumour centre where care is taken to avoid contaminating uninvolved muscle compartments and the surgeon made aware of the path taken, so that the biopsy tract can be resected at the time of definitive surgery. Wide field of view T1-weighted

Figure 4 **Anterioposterior (AP) plain radiograph in a patient with EFT of the distal right tibia, demonstrating a lucent lesion with associated lamellated 'onion skin' periosteal reaction (short arrow) and a Codman triangle (arrow head).**

Figure 5 **Selected slice from wide field of view coronal T1-weighted MRI (TR 439, TE 14 ms) of the same patient as Fig. 3. Note intermediate signal intramedullary tumour (arrow) replacing the normal fatty marrow signal seen contralaterally.**

images should be performed as part of the staging MR to evaluate the remainder of the bone in which the primary tumour arises for 'skip lesions' and the contralateral side to assess for metastases (Fig. 5). Chest CT and bone scintigraphy complete the staging investigations, with the aim of identifying metastatic disease. Approximately 10–15% of patients with OS have metastatic disease at diagnosis, usually within the lungs or other bones[28] and approximately 25% of patients with EFTs present with metastases, usually lung metastases[29].

Modern chemotherapeutic and surgical techniques enable approximately 90% of patients to undergo limb-salvage surgery rather than amputation[30], with surgery taking place after induction chemotherapy. Following resection the specimen is histologically graded according to the degree of necrosis present. The degree of tumour necrosis following induction chemotherapy is an important factor in determining outcome[31], with greater than 90% necrosis being a predictor of favourable outcome[32]. Narrow surgical margins and low necrosis levels following chemotherapy are associated with an increased risk of local recurrence[33]. Given that the degree of necrosis present has an effect on the probable outcome, yet is not possible to assess before surgery using conventional imaging modalities, there have been efforts to find novel techniques that may be able to determine the level of necrosis before surgery, which in turn may allow modification to treatment in those patients with a low necrosis fraction following induction.

The concept of using DWI in OS is not new. Lang *et al*. first described the use of DWI to assess tumour necrosis in a rat model for OS in 1998[34]. A recent clinical study evaluated change in pre- and post-treatment tumour volumes, ADC values, static post-gadolinium signal intensity on T1-weighted images and contrast to noise ratios on T2-weighted images in a cohort of patients with OS and EFTs divided into 2 groups; those with >90% tumour

necrosis and those with <90% necrosis[35]. Of all the parameters studied, only the change in ADC pre- and post-induction showed a statistically significant difference between the 2 groups. Despite Hayashida *et al.*[35] finding no difference in changes of static post-contrast signal intensity between the 2 groups, many other research groups have evaluated dynamic MR contrast enhancement both in relation to event-free survival[36] and compared with necrosis measured histologically[37]. Reddick *et al.*[36] describe a dual compartment model of dynamic contrast enhancement as a measure of regional contrast access to the tumour, with lower levels of regional contrast access and smaller size of the tumour being associated with a better prognosis. Dyke *et al.*[37] found that histograms for both the initial slope of contrast enhancement and dual compartment pharmacokinetic model of dynamic MR enhancement predicted the pathologic tumour necrosis level in patients with OS and EFT imaged following induction chemotherapy, before surgery. The investigators suggest that this technique could be used serially during chemotherapy to identify those patients who may be inadequately responding (i.e. those not achieving >90% necrosis) so that a modification of therapy could be considered; however currently there are no studies evaluating the changes in dynamic MR contrast curves during chemotherapy, which are necessary to determine what MR parameters, if any, predict a necrosis fraction of less than 90% at the end of induction. Being able to identify inadequate response during treatment would enable modification during induction treatment, rather than modifying the post-induction, pre-surgical phase of management. Further work in this area is needed.

Functional assessment of osteosarcoma using PET has also been compared with histopathologic necrosis grade. Ye *et al.*[38] compared SUV_{max} and tumour to background ratios (TBR) obtained pre- and post-induction chemotherapy with histologic necrosis at surgery, reporting that tumour background ratio after treatment and the ratio $TBR_{post\text{-}induction}/TBR_{pre\text{-}induction}$ showed a statistically significant correlation with the degree of necrosis. SUV_{max}, the most commonly measured parameter in PET, did not show a significant correlation with necrosis fraction.

There have been limited reports of magnetic resonance spectroscopy (MRS) being utilised to evaluate musculoskeletal tumour metabolism. Wang *et al.*[39] and Fayad *et al.*[40] have both demonstrated increased choline peaks within malignant bone tumours compared with benign lesions, using single voxel[39] and multivoxel MRS techniques[40] at 1.5 T. The feasibility of MRS for musculoskeletal lesions at 3 T has also been demonstrated [41]. The observed elevated choline peak is believed to reflect the presence of glycerophosphocholine and phosphocholine in addition to choline. These substances are utilised in the synthesis and degradation of cell walls and hence it is postulated that increased cell turnover seen in malignant lesions leads to higher levels than those seen in benign lesions. To our knowledge there are no studies evaluating longitudinal MRS choline peak measurements in malignant musculoskeletal lesions during treatment to assess for change in the spectra obtained, nor the possible prognostic value of such measurements.

Germ cell tumours (GCT)

There is a significant increase in the incidence of gonadal GCTs amongst adolescents and young adults. This has been reported to increase from 0.22 per 100,000 in 12–14 year olds to 1.18 in 15–19 year olds and to 3.5 in 20–24 year olds[7], with testicular GCTs contributing almost entirely to the increase in incidence. The adolescent trends of non-gonadal GCT are less well documented. There is a small decrease in the incidence of intracranial GCT with age, and there is a slight increase in the incidence of other extragonadal sites[7].

GCTs occur most frequently in the gonads (80–90%). Extragonadal locations also occur in 5–10% of cases, usually in or near the midline[42]. The mediastinum is the most common extragonadal location (Fig. 6), representing 50–70% of extragonadal GCTs[43]. Retroperitoneal tumours are the second most common (30–40%), followed by intracranial tumours (1–5%), with a predilection for the pineal and the suprasellar regions[44]. Sacrococcygeal GCTs and extragonadal germ cell cancer syndrome are rare entities in adolescence[43].

Testicular GCTs are classified from their histologic features into seminomas and non-seminomas. Seminomas account for about 40% of GCTs, of which classic and anaplastic cell types constitute the majority. The rest are classified as spermatocytic.

Figure 6 **Axial contrast-enhanced CT section of a mediastinal germ cell tumour demonstrating a large heterogeneous anterior mediastinal mass, containing areas of fat (short arrow) and calcification (arrow head).**

Non-seminomas account for about 60% of GCTs. Non-seminomas occur in patients aged 15–35 years. Lymphatic and vascular invasion is associated with a higher rate of relapse and predicts occult nodal metastases[43].

Ovarian GCTs account for more than half of all ovarian tumours in childhood and adolescence, with approximately one-third being malignant. The most common histologic type of malignant tumour is dysgerminoma, with immature teratoma, choriocarcinoma, embryonal carcinoma and endodermal sinus tumours being the other types observed.

Imaging of GCTs

The diagnosis of GCTs is based on a combination of clinical examination, evaluation of biochemical tumour markers (α-fetoprotein (AFP), human chorionic gonadotropin (HCG) and lactate dehydrogenase (LDH)) and imaging investigations.

Ultrasonography of the testes is mandatory in gonadal GCTs, to diagnose, distinguish from other scrotal pathologies and assess the contralateral testis. The tumours are usually hypoechoeic compared with the normal testis, although varied degrees of increased echogenicity have also been described. These tumours may present as multifocal lesions or diffuse infiltration causing subtle alteration in testicular echotexture[46].

CT of the chest, abdomen and pelvis with oral and intravenous contrast is required for staging and follow-up, to evaluate for nodal metastases and to assess for intra-abdominal spread in the setting of ovarian tumours. It has been suggested that patients who have stage I testicular tumours (limited to the testis, epididymis or spermatic cord) can have a chest radiograph as an alternative to CT of the chest for surveillance[47–49]. There are limitations to the use of CT in staging. It should be noted that pulmonary/pleural nodules of <1 cm can represent a false–positive finding.

Interpretation of lymph nodes based on morphology and size on CT scans of the abdomen and pelvis can also be difficult and might give false-negative results in up to 30% of cases, making the differentiation between stages I and IIA (retroperitoneal node involvement <2cm diameter) unreliable[47,49,50].

Evaluation of the retroperitoneum is best performed using CT, which is more sensitive than ultrasound in assessing the size and extent of the disease[51]. Ultrasonography in staging is reserved for the evaluation of solid organ involvement such as the liver and spleen[47,48].

A report of the European Germ Cell Cancer Consensus Group (EGCCCG), advised that MRI scans of the abdomen and pelvis should be restricted to patients to whom intravenous contrast media cannot be given as MRI does not provide additional information[52]; however, there is emerging evidence that MRI is useful in the detection and characterisation of CNS, musculoskeletal and hepatic metastases and demonstration of inferior vena cava (IVC) tumour invasion, enteric fistulae and vascular anatomy in patients before retroperitoneal lymph node surgery[53,54]. There is also some evidence that lymphotrophic nanoparticle-enhanced MRI (LNMRI) demonstrates higher sensitivity and specificity for detecting nodal metastases compared with unenhanced MRI and CT[55], although the numbers of patients in this study were small and more work is needed in this area.

The role of PET-CT in GCT is controversial. The EGCCCG advised that PET scans are not to be used outside clinical trials as part of routine initial staging procedures. However, PET-CT may also have a role in routine clinical practice. For initial staging, there is some evidence that PET-CT may be helpful in detecting involved nodes less than 2 cm in diameter (which would upstage to IIA) in otherwise apparently stage I non-seminomatous disease[56,57]. There are also several studies that advocate the use of PET-CT for follow-up as it can detect residual disease in post-chemotherapy seminoma and differentiate between fibrosis and recurrence, particularly when there is a discrepancy between tumour markers and imaging changes[58]. The role of PET-CT as a predictor of response is less clear in the literature[59].

Bone scans should be performed in patients with elevated levels of alkaline phosphatase or if bone metastases are clinically suspected.

Carcinoma

The incidence rates for carcinoma increase with increasing age. Head and neck cancers are the commonest in 12–14 year olds and 15–19 year olds. However, these only make up 24% of all carcinomas in 20–24 year olds. The thyroid is the commonest site followed by nasopharyngeal carcinoma, which is very rare in the United Kingdom[7].

Carcinomas typically seen in adults are rare in adolescents but show a steady increase with increasing age. This is particularly observed in the genito-urinary tract with invasive cervical and uterine carcinoma contributing to the largest increase. Gastro-intestinal malignancy seen in adolescents mainly involves the colon and rectum[7].

Thyroid carcinoma

Thyroid carcinoma in adolescents differs from adult onset thyroid cancer in its presentation and clinical course. It usually presents with bulkier tumour disease, greater incidence of lymph node and pulmonary metastases and also has a higher recurrence rate[60]. However, it tends to have an excellent prognosis.

It is estimated that the tumour involves both lobes of the thyroid in 20–49%. Cervical lymph node involvement is observed in 60–90% at the time of presentation[60].

Reports vary as to the incidence of pulmonary metastases varying between 6 and 33%[61].

Papillary carcinoma is the commonest histologic type (60%), followed by follicular variant of papillary carcinoma (20%) and pure follicular in 5%. Medullary thyroid carcinoma is very rare and is confined to patients with multiple endocrine neoplasia type 2A and 2B[60]. Predictors for increased recurrence rate include capsular invasion, soft-tissue invasion, positive tumour margins and the location of the tumour[60].

Imaging of thyroid carcinoma is performed using ultrasonography to characterise the lesion and evaluate local lymph nodes. Ultrasonography is useful in differentiating solid from cystic lesions and revealing non-palpable lesions. Cystic lesions are usually considered to be benign; a solid nodule is more likely to be malignant. However, up to 50% of malignant lesions may have a cystic component, and approximately 8% of cystic lesions represent malignancies[62]. Benign features on ultrasound include multiple, solid isoechogenic or non-echogenic lesions and a uniform peripheral halo[62]. Malignant features include a thick irregular halo, microcalcification (Fig. 7), and marked hypoechogenicity (compared with the normal thyroid tissue). Colour Doppler sonography is valuable in distinguishing a cystic lesion (with no vascular flow) from a solid neoplasm (with intranodular flow)[63]. Suspicious lesions should undergo fine-needle aspiration for histologic diagnosis[64].

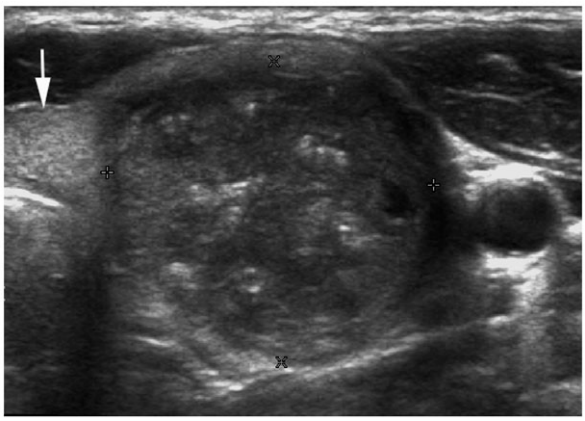

Figure 7 **Transverse ultrasound image of the left lobe of the thyroid and isthmus (short arrow). The left lobe of the thyroid contains a heterogeneous echogenicity nodule, with multiple small foci of calcification (between callipers). Fine-needle aspiration revealed papillary thyroid carcinoma.**

Non-contrast CT is used for evaluation of substernal extension, local invasion, lymph node and pulmonary metastasis. The CT lung findings of metastatic disease include diffuse milliary nodules or, less often, infiltrating nodules[65].

Thyroid scintigraphy has not proven worthwhile in distinguishing malignant from benign disease. Classic hot spots are associated with about a 6% incidence of malignancy[66]. Cold nodules are usually benign adenomas, although, in children, a larger number of these are carcinomas[66]. Solid lesions that are cold on scintigraphy are malignant in about 30% of cases[67]. Untreated hot nodules can progress to carcinoma[68]. Surgical treatment is advisable for all children and adolescents with autonomously functioning thyroid nodules because of the risks of hyperthyroidism and thyroid carcinoma[68]. Total-body radioactive iodine scans often reveal pulmonary or nodal metastases, which are not visualised on CT[61].

Nasopharyngeal carcinoma

Nasopharyngeal carcinoma (NPC) is a tumour arising from the epithelial cells that cover the surface and line

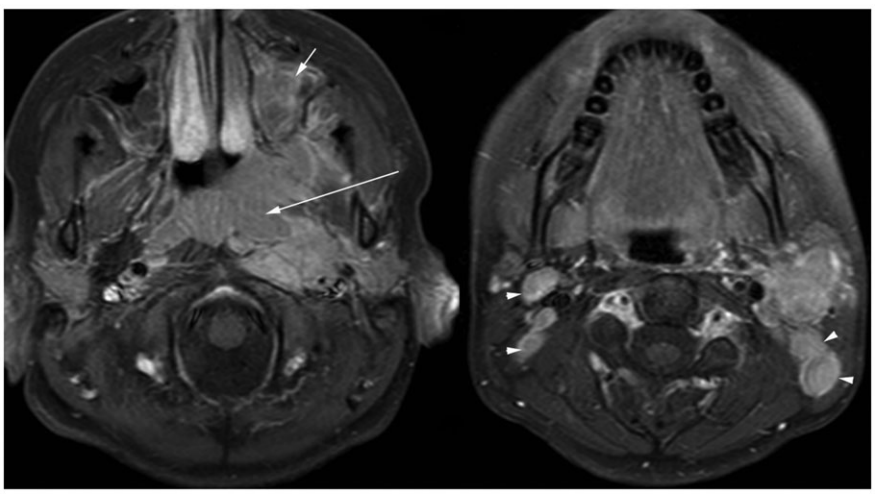

Figure 8 **Axial contrast-enhanced fat-saturated T1-weighted MRI (TR 567, TE 12 ms) of a patient with nasopharyngeal carcinoma (long arrow) invading the left parapharyngeal space, parotid and left maxillary antrum (short arrow), with multiple lymph node metastases (arrow heads).**

the nasopharynx. The annual incidence of NPC in the United Kingdom is 0.3 per million at age 0–14 years, and 1–2 per million at age 15–19 years, with higher incidence in the oriental population[69].

Three subtypes of NPC are recognised in the World Health Organization (WHO) classification: squamous cell carcinoma, typically found in the older adult population, non-keratinizing carcinoma and undifferentiated carcinoma. Approximately one-third of nasopharyngeal carcinomas of the undifferentiated type are diagnosed in adolescents or young adults[69].

NPC usually originates in the lateral wall of the nasopharynx, which includes the fossa of Rosenmüller. It can extend to the opposite lateral wall and postero-superiorly to the base of the skull or the palate, nasal cavity or oropharynx. It then typically metastasizes to cervical lymph nodes, which can be the initial presentation in many patients (Fig. 8). Distant metastases may occur in bone, lung, mediastinum and, more rarely, the liver.

Imaging features of NPC on CT and MRI in adolescents and young adults differ from those in the elderly. It usually presents as a homogeneous enhancing mass lesion in the nasopharynx, which is isointense to slightly hyperintense (relative to muscles) on T1- and T2-weighted images[70,71]. Local invasion and cervical lymph node involvement, which occurs in 80–90% of cases, are also common but tend to be homogeneous without evidence of necrosis on CT[70–72].

The differential diagnosis of NPC includes lymphoma, juvenile angiofibroma and rhabdomyosarcoma. Juvenile angiofibroma is usually easily diagnosed on CT and MRI because of its avid enhancement and flow voids on MRI. Rhabdomysarcoma tends to be heterogeneous in signal intensity. Lymphoma tends to have a particularly high T2 signal intensity. The pattern of local invasion can also differentiate NPC from other possible diagnoses. It tends to be aggressive and destructive, involving the skull base in 80%, which is only observed in 18% of rahbdomyosarcomas[71,72]. Lymphoma usually causes permeative bone destruction and invades the skull base through the foramina[71,72].

Conclusion

The spectrum of malignancy seen during adolescence and early adulthood is unlike that seen at any other time in life. Close working relationships between those involved in imaging adolescent oncology patients (be they paediatric radiologists or 'adult' radiologists with special interests in particular body parts or tumour types) and clinical colleagues, as part of a wider multidisciplinary team, is essential to provide a coherent adolescent oncology imaging service. Further research towards a greater understanding and characterisation of pathologic processes and treatment change that may help risk stratify adolescent patients is needed. This may help improve outcomes, which hitherto have lagged behind both adult and paediatric patients.

References

[1] National Collaborating Centre for Cancer. Improving outcomes in children and young people with cancer. London (UK): National Institute for Health and Clinical Excellence (NICE); 2005, 194 p.

[2] Bleyer WA, Montello M, Budd T, Kelahan A, Ries L. US cancer incidence, mortality and survival: young adults are lagging further behind. Proc Am Soc Clin Oncol 2002; 21: 389.

[3] Stiller C. Epidemiology of cancer in adolescents. Med Pediatr Oncol 2002; 39: 149–55. doi:10.1002/mpo.10142. PMid:12210442.

[4] Ries LAG, Eisner MP, Kosary CL, *et al.* SEER cancer statistics review, 1973–1998. Bethesda, MD: National Cancer Institute; 2001.

[5] Cotterill SJ, Parker L, Malcolm AJ, Reid M, More L, Craft AW. Incidence and survival for cancer in children and young adults in the North of England, 1968–1995: a report from the Northern Region Young Persons' Malignant Disease Registry. Br J Cancer 2000; 83: 397–403. doi:10.1054/bjoc.2000.1313. PMid:10917558.

[6] Michelagnoli MP, Pritchard J, Phillips MB. Adolescent oncology – a homeland for the 'lost tribe'. Eur J Cancer 2003; 39: 2571–2. doi:10.1016/j.ejca.2003.09.012. PMid:14642918.

[7] Birch JM, Alston RD, Quinn M, Kelsey AM. Incidence of malignant disease by morphological type, in young persons aged 12–24 years in England, 1979–1997. Eur J Cancer 2003; 39: 2622–31. doi:10.1016/j.ejca.2003.08.006. PMid:14642924.

[8] Wright D, McKeever P, Carter R. Childhood non-Hodgkin lymphomas in the United Kingdom: findings from the UK Children's Cancer Study Group. J Clin Pathol 1997; 50: 128–34. doi:10.1136/jcp.50.2.128. PMid:9155693.

[9] White KS. Thoracic imaging of pediatric lymphomas. J Thorac Imaging 2001; 16: 224–37. doi:10.1097/00005382-200110000-00004. PMid:11685088.

[10] Sheth S, Fishman EK. Non-Hodgkin lymphoma: pattern of disease at spiral CT. Crit Rev Diagn Imaging 2001; 42: 307–56.

[11] Murphy SB. Classification, staging and end results of treatment of childhood non-Hodgkin's lymphomas: dissimilarities from lymphomas in adults. Semin Oncol 1980; 7: 332–9.

[12] Moog F, Bangerter M, Diederichs CG, *et al.* Lymphoma: role of whole-body 2-deoxy-2-[F-18]fluoro-D-glucose (FDG) PET in nodal staging. Radiology 1997; 203: 795–800.

[13] Hoh CK, Glaspy J, Rosen P, *et al.* Whole-body FDG-PET imaging for staging of Hodgkin's disease and lymphoma. J Nucl Med 1997; 38: 343–8.

[14] Jerusalem G, Warland V, Najjar F, *et al.* Whole-body ^{18}F-FDG PET for the evaluation of patients with Hodgkin's disease and non-Hodgkin's lymphoma. Nucl Med Commun 1999; 20: 13–20.

[15] Canini R, Battista G, Monetti N, *et al.* [Bulky mediastinal lymphomas: role of magnetic resonance and SPECT-Ga-67 in the evaluation of residual masses]. Radiol Med 1995; 90: 448–56. (in Italian).

[16] Bergin CJ, Healy MV, Zincone GE, Castellino RA. MR evaluation of chest wall involvement in malignant lymphoma. J Comput Assist Tomogr 1990; 14: 928–32.

[17] Humphries P, Punwani S, Prakash V, *et al.* Comparison of whole-body STIR-HASTE and ^{18}FDG-PET/CT for staging paediatric lymphoma. Pediatr Radiol 2008; 38(Suppl 3): S558.

[18] Pipe JG. Motion correction with PROPELLER MRI: application to head motion and free-breathing cardiac imaging. Magn Reson Med 1999; 42: 963–9. doi:10.1002/(SICI)1522-2594(199911)42:5<963::AID-MRM17>3.0.CO;2-L. PMid:10542356.

[19] Siniluoto TM, Tikkakoski TA, Lahde ST, Paivansalo MJ, Koivisto MJ. Ultrasound or CT in splenic diseases? Acta Radiol 1994; 35: 597–605.
[20] Lauenstein TC, Semelka RC. Emerging techniques: whole-body screening and staging with MRI. J Magn Reson Imaging 2006; 24: 489–98. doi:10.1002/jmri.20666. PMid:16888774.
[21] Daldrup-Link HE, Franzius C, Link TM, *et al.* Whole-body MR imaging for detection of bone metastases in children and young adults: comparison with skeletal scintigraphy and FDG PET. AJR Am J Roentgenol 2001; 177: 229–36.
[22] Rigo P, Paulus P, Kaschten BJ, *et al.* Oncological applications of positron emission tomography with fluorine-18 fluorodeoxyglucose. Eur J Nucl Med 1996; 23: 1641–74. doi:10.1007/BF01249629. PMid:8929320.
[23] Newman JS, Francis IR, Kaminski MS, Wahl RL. Imaging of lymphoma with PET with 2-[F-18]-fluoro-2-deoxy-D-glucose: correlation with CT. Radiology 1994; 190: 111–6.
[24] Hutchings M, Loft A, Hansen M, *et al.* FDG-PET after two cycles of chemotherapy predicts treatment failure and progression-free survival in Hodgkin lymphoma. Blood 2006; 107: 52–9. doi:10.1182/blood-2005-06-2252. PMid:16150944.
[25] Zacharia TT, Law M, Naidich TP, Leeds NE. Central nervous system lymphoma characterization by diffusion-weighted imaging and MR spectroscopy. J Neuroimaging 2008; 18: 411–7.
[26] Humphries PD, Sebire NJ, Siegel MJ, Olsen OE. Tumors in pediatric patients at diffusion-weighted MR imaging: apparent diffusion coefficient and tumor cellularity. Radiology 2007; 245: 848–54. doi:10.1148/radiol.2452061535. PMid:17951348.
[27] Punwani S, Prakash V, Bandula S, *et al.* Correlation of lymph node derived apparent diffusion coefficient (ADC) and PET/CT determined specific uptake value (SUV) in paediatric lymphoma. Pediatr Radiol 2008; 38(Suppl 3): S534–69.
[28] Kager L, Zoubek A, Potschger U, *et al.* Primary metastatic osteosarcoma: presentation and outcome of patients treated on neoadjuvant Cooperative Osteosarcoma Study Group protocols. J Clin Oncol 2003; 21: 2011–8. doi:10.1200/JCO.2003.08.132. PMid:12743156.
[29] Paulussen M, Frohlich B, Jurgens H. Ewing tumour: incidence, prognosis and treatment options. Paediatr Drugs 2001; 3: 899–913. doi:10.2165/00128072-200103120-00003. PMid:11772151.
[30] Weis LD. The success of limb-salvage surgery in the adolescent patient with osteogenic sarcoma. Adolesc Med 1999; 10: 451–8, xii.
[31] Meyers PA, Gorlick R, Heller G, *et al.* Intensification of preoperative chemotherapy for osteogenic sarcoma: results of the Memorial Sloan-Kettering (T12) protocol. J Clin Oncol 1998; 16: 2452–8.
[32] Wunder JS, Paulian G, Huvos AG, Heller G, Meyers PA, Healey JH. The histological response to chemotherapy as a predictor of the oncological outcome of operative treatment of Ewing sarcoma. J Bone Joint Surg Am 1998; 80: 1020–33.
[33] Gherlinzoni F, Picci P, Bacci G, Campanacci D. Limb sparing versus amputation in osteosarcoma. Correlation between local control, surgical margins and tumor necrosis: Istituto Rizzoli experience. Ann Oncol 1992; 3(Suppl 2): S23–7.
[34] Lang P, Wendland MF, Saeed M, *et al.* Osteogenic sarcoma: noninvasive in vivo assessment of tumor necrosis with diffusion-weighted MR imaging. Radiology 1998; 206: 227–35.
[35] Hayashida Y, Yakushiji T, Awai K, *et al.* Monitoring therapeutic responses of primary bone tumors by diffusion-weighted image: Initial results. Eur Radiol 2006; 16: 2637–43. doi:10.1007/s00330-006-0342-y. PMid:16909220.
[36] Reddick WE, Wang S, Xiong X, *et al.* Dynamic magnetic resonance imaging of regional contrast access as an additional prognostic factor in pediatric osteosarcoma. Cancer 2001; 91: 2230–7. doi:10.1002/1097-0142(20010615)91:12<2230::AID-CNCR1253>3.3.CO;2-K. PMid:11413510.
[37] Dyke JP, Panicek DM, Healey JH, *et al.* Osteogenic and Ewing sarcomas: estimation of necrotic fraction during induction chemotherapy with dynamic contrast-enhanced MR imaging. Radiology 2003; 228: 271–8. doi:10.1148/radiol.2281011651. PMid:12832588.
[38] Ye Z, Zhu J, Tian M, *et al.* Response of osteogenic sarcoma to neoadjuvant therapy: evaluated by ^{18}F-FDG-PET. Ann Nucl Med 2008; 22: 475–80. doi:10.1007/s12149-008-0147-y. PMid:18670853.
[39] Wang CK, Li CW, Hsieh TJ, Chien SH, Liu GC, Tsai KB. Characterization of bone and soft-tissue tumors with in vivo 1H MR spectroscopy: initial results. Radiology 2004; 232: 599–605. doi:10.1148/radiol.2322031441. PMid:15286325.
[40] Fayad LM, Bluemke DA, McCarthy EF, Weber KL, Barker PB, Jacobs MA. Musculoskeletal tumors: use of proton MR spectroscopic imaging for characterization. J Magn Reson Imaging 2006; 23: 23–8. doi:10.1002/jmri.20448. PMid:16315208.
[41] Fayad LM, Barker PB, Jacobs MA, *et al.* Characterization of musculoskeletal lesions on 3-T proton MR spectroscopy. AJR Am J Roentgenol 2007; 188: 1513–20. doi:10.2214/AJR.06.0935. PMid:17515370.
[42] Nichols CR. Testicular cancer. Curr Probl Cancer 1998; 22: 187–274. doi:10.1016/S0147-0272(98)90012-5. PMid:9743088.
[43] Nichols CR, Fox EP. Extragonadal and pediatric germ cell tumors. Hematol Oncol Clin North Am 1991; 5: 1189–209.
[44] Takeda S, Miyoshi S, Ohta M, Minami M, Masaoka A, Matsuda H. Primary germ cell tumors in the mediastinum: a 50-year experience at a single Japanese institution. Cancer 2003; 97: 367–76. doi:10.1002/cncr.11068. PMid:12518361.
[45] International Germ Cell Consensus Classification: a prognostic factor-based staging system for metastatic germ cell cancers.International Germ Cell Cancer Collaborative Group. J Clin Oncol 1997; 15: 594–603.
[46] Tessler FN, Tublin ME, Rifkin MD. Ultrasound assessment of testicular and paratesticular masses. J Clin Ultrasound 1996; 24: 423–36. doi:10.1002/(SICI)1097-0096(199610)24:8<423::AID-JCU3>3.0.CO;2-M. PMid:8884520.
[47] White PM, Adamson DJ, Howard GC, Wright AR. Imaging of the thorax in the management of germ cell testicular tumours. Clin Radiol 1999; 54: 207–11. doi:10.1016/S0009-9260(99)91152-2. PMid:10210337.
[48] Meyer CA, Conces DJ. Imaging of intrathoracic metastases of nonseminomatous germ cell tumors. Chest Surg Clin N Am 2002; 12: 717–38.
[49] See WA, Hoxie L. Chest staging in testis cancer patients: imaging modality selection based upon risk assessment as determined by abdominal computerized tomography scan results. J Urol 1993; 150: 874–8.
[50] White PM, Howard GC, Best JJ, Wright AR. The role of computed tomographic examination of the pelvis in the management of testicular germ cell tumours. Clin Radiol 1997; 52: 124–9. doi:10.1016/S0009-9260(97)80105-5. PMid:9043046.
[51] Leibovitch L, Foster RS, Kopecky KK, Donohue JP. Improved accuracy of computerized tomography based clinical staging in low stage nonseminomatous germ cell cancer using size criteria of retroperitoneal lymph nodes. J Urol 1995; 154: 1759–63. doi:10.1016/S0022-5347(01)66778-8. PMid:7563341.
[52] McLeod DG, Weiss RB, Stablein DM, *et al.* Staging relationships and outcome in early stage testicular cancer: a report from the Testicular Cancer Intergroup Study. J Urol 1991; 145: 1178–83.
[53] Dalal PU, Sohaib SA, Huddart R. Imaging of testicular germ cell tumours. Cancer Imaging 2006; 6: 124–34. doi:10.1102/1470-7330.2006.0020. PMid:16966068.
[54] Bellin MF, Roy C, Kinkel K, *et al.* Lymph node metastases: safety and effectiveness of MR imaging with ultrasmall superparamagnetic iron oxide particles – initial clinical experience. Radiology 1998; 207: 799–808.
[55] Harisinghani MG, Saksena M, Ross RW, *et al.* A pilot study of lymphotrophic nanoparticle-enhanced magnetic resonance

imaging technique in early stage testicular cancer: a new method for noninvasive lymph node evaluation. Urology 2005; 66: 1066–71. doi:10.1016/j.urology.2005.05.049. PMid:16286125.

[56] Lassen U, Daugaard G, Eigtved A, *et al.* Wholebody positron emission tomography (PET) with FDG in patients with stage I non-seminomatous germ cell tumours (NSGCT). Eur J Nucl Med Imaging 2003; 30: 396–402.

[57] Albers P, Bender H, Yilmaz H, Schoeneich G, Biersack HJ, Mueller SC. Positron emission tomography in the clinical staging of patients with stage I and II testicular germ cell tumors. Urology 1999; 53: 808–11. doi:10.1016/S0090-4295(98)00576-7. PMid:10197862.

[58] Cremerius U, Wildberger JE, Borchers H, *et al.* Does positron emission tomography using 18-fluoro-2-deoxyglucose improve clinical staging of testicular cancer? Results of a study in 50 patients. Urology 1999; 54: 900–4. doi:10.1016/S0090-4295(99)00272-1. PMid:10565755.

[59] Tsatalpas P, Beuthien-Baumann B, Kropp J, *et al.* Diagnostic value of ^{18}F-FDG positron emission tomography for detection and treatment control of malignant germ cell tumors. Urol Int 2002; 68: 157–63. doi:10.1159/000048442. PMid:11919460.

[60] Farahati J, Parlowsky T, Mader U, Reiners C, Bucsky P. Differentiated thyroid cancer in children and adolescents. Langenbecks Arch Surg 1998; 383: 235–9. doi:10.1007/s004230050124.

[61] Samuel AM, Rajashekharrao B, Shah DH. Pulmonary metastases in children and adolescents with well-differentiated thyroid cancer. J Nucl Med 1998; 39: 1531–6.

[62] Hoang JK, Lee WK, Lee M, Johnson D, Farrell S. US features of thyroid malignancy: pearls and pitfalls. Radiographics 2007; 27: 847–60. doi:10.1148/rg.273065038. PMid:17495296.

[63] Lyshchik A, Drozd V, Demidchik Y, Reiners C. Diagnosis of thyroid cancer in children: value of gray-scale and power doppler US. Radiology 2005; 235: 604–13. doi:10.1148/radiol.2352031942. PMid:15770036.

[64] Khurana KK, Labrador E, Izquierdo R, Mesonero CE, Pisharodi LR. The role of fine-needle aspiration biopsy in the management of thyroid nodules in children, adolescents, and young adults: a multi-institutional study. Thyroid 1999; 9: 383–6. doi:10.1089/thy.1999.9.383. PMid:10319945.

[65] Festen C, Otten BJ, van de Kaa CA. Follicular adenoma of the thyroid gland in children. Eur J Pediatr Surg 1995; 5: 262–4. doi:10.1055/s-2008-1066220. PMid:8555125.

[66] Geiger JD, Thompson NW. Thyroid tumors in children. Otolaryngol Clin North Am 1996; 29: 711–9.

[67] Desjardins JG, Khan AH, Montupet P, *et al.* Management of thyroid nodules in children: a 20-year experience. J Pediatr Surg 1987; 22: 736–9. doi:10.1016/S0022-3468(87)80616-4. PMid:3656022.

[68] Harach HR, Sanchez SS, Williams ED. Pathology of the autonomously functioning (hot) thyroid nodule. Ann Diagn Pathol 2002; 6: 10–9. doi:10.1053/adpa.2002.30605. PMid:11842375.

[69] Brennan B. Nasopharyngeal carcinoma. Orphanet J Rare Dis 2006; 1: 23. doi:10.1186/1750-1172-1-23. PMid:16800883.

[70] Yabuuchi H, Fukuya T, Murayama S, *et al.* CT and MR features of nasopharyngeal carcinoma in children and young adults. Clin Radiol 2002; 57: 205–10. doi:10.1053/crad.2001.0731. PMid:11952316.

[71] Stambuk HE, Patel SG, Mosier KM, Wolden SL, Holodny AI. Nasopharyngeal carcinoma: recognizing the radiographic features in children. AJNR Am J Neuroradiol 2005; 26: 1575–9.

[72] Chin SC, Fatterpekar G, Chen CY, Som PM. MR imaging of diverse manifestations of nasopharyngeal carcinomas. AJR Am J Roentgenol 2003; 180: 1715–22.